Published in final edited form as:
J Biomech. 2012 March 15; 45(5): 799–804. doi:10.1016/j.jbiomech.2011.11.020.

Persistent vascular collagen accumulation alters hemodynamic recovery from chronic hypoxia

Diana M. Tabima[1], **Alejandro Roldan-Alzate**[1], **Zhijie Wang**[1], **Timothy A. Hacker**[2], **Robert C. Molthen**[3], and **Naomi C. Chesler**[1,2]

[1]Department of Biomedical Engineering, University of Wisconsin-Madison, Madison, WI 53706-1609

[2]Department of Medicine, University of Wisconsin-Madison, Madison, WI 53706-1609

[3]Department of Medicine-PCC, Medical College of Wisconsin, Milwaukee, WI 53201

Abstract

Pulmonary arterial hypertension (PAH) is caused by narrowing and stiffening of the pulmonary arteries that increase pulmonary vascular impedance (PVZ). In particular, small arteries narrow and large arteries stiffen. Large pulmonary artery (PA) stiffness is the best current predictor of mortality from PAH. We have previously shown that collagen accumulation leads to extralobar PA stiffening at high strain (Ooi, Wang et al. 2010). We hypothesized that collagen accumulation would increase PVZ, including total pulmonary vascular resistance (Z_0), characteristic impedance (Z_C), pulse wave velocity (PWV), and index of global wave reflections (P_b/P_f), which contribute to increased right ventricular afterload. We tested this hypothesis by exposing mice unable to degrade type I collagen ($Col1a1^{R/R}$) to 21 days of hypoxia (hypoxia), some of which were allowed to recover for 42 days (recovery). Littermate wild-type mice ($Col1a1^{+/+}$) were used as controls. In response to hypoxia, mean PA pressure (mPAP) increased in both mouse genotypes with no changes in cardiac output (CO) or PA inner diameter (ID); as a consequence, Z_0 (mPAP/CO) increased by ~100% in both genotypes ($p<0.05$). Contrary to our expectations, Z_C, PWV and P_b/P_f did not change. However, with recovery, Z_C and PWV decreased in the $Col1a1^{+/+}$ mice and remained unchanged in the $Col1a1^{R/R}$ mice. Z_0 decreased with recovery in both genotypes. Microcomputed tomography measurements of large PAs did not show evidence of stiffness changes as a function of hypoxia exposure or genotype. We conclude that hypoxia-induced PA collagen accumulation does not affect the pulsatile components of pulmonary hemodynamics but that excessive collagen accumulation does prevent normal hemodynamic recovery, which may have important consequences for right ventricular function.

Introduction

Pulmonary hypertension (PH) is a family of diseases that includes pulmonary arterial hypertension (PAH), pulmonary hypertension associated with hypoxia and/or lung diseases, pulmonary hypertension secondary to left heart disease, chronic thromboembolic disease

Contact Information: Naomi C. Chesler, Ph.D., Associate Professor of Biomedical Engineering, University of Wisconsin at Madison, 2146 Engineering Centers Building, 1550 Engineering Drive, Madison, Wisconsin, 53706-1609, tel: 608 265-8920, Fax: 608 265-9239, chesler@engr.wisc.edu.

and pulmonary hypertension associated with other "miscellaneous" diseases (e.g., scleroderma, sarcoidosis, lymphangiomatosis and histiocytosis X) (Simonneau, Galie et al. 2004). Hypoxic pulmonary hypertension (HPH) is caused by alveolar hypoxia and can result from living at high altitudes and/or diseases related to the lung, including chronic obstructive pulmonary disease (COPD), cystic fibrosis and obstructive sleep apnea.

Many structural changes occur in the vasculature as a result of PH including intimal thickening and fibrosis, medial hypertrophy, muscularization of previously non-muscularized arteries, adventitial proliferation and increased extracellular matrix (ECM) deposition (Stenmark and Mecham 1997; Kobs and Chesler 2006; Stenmark, Davie et al. 2006; Stenmark, Fagan et al. 2006; Tuchscherer, Vanderpool et al. 2007). Functional changes occur as well, including increased large pulmonary artery (PA) stiffening (Kobs, Muvarak et al. 2005; Kobs and Chesler 2006; Tabima and Chesler 2010). In recent work, our group showed that collagen plays an important role in HPH-induced PA stiffening (Ooi, Wang et al. 2010). In particular, we used a mouse model in which collagen type I is resistant to collagenase degradation ($Col1a1^{R/R}$) to show that persistently high PA collagen content after recovery from chronic hypoxia causes persistent PA stiffening, independent of changes in elastin or smooth muscle cell tone (Ooi, Wang et al. 2010).

Vascular collagen content and its impact on hemodynamics is especially relevant to scleroderma, or progressive systemic sclerosis (SSc), a disease of unknown etiology characterized by overproduction of collagen throughout the body (Cotran, Kuman et al. 1999). Two thirds of patients with SSc have pathological evidence of pulmonary vascular disease (Salerni, Rodnan et al. 1977; Young and Mark 1978). PAH is present in up to 33% of patients with diffuse SSc and 60% of patients with limited SSc (CREST) (Fagan and Badesch 2002) and right ventricular failure secondary to PAH is the most common cardiac complication of SSc (Silver 1996). Furthermore, SSc-PAH patients have an especially poor response to standard therapy, resulting in high mortality (Coghlan and Mukerjee 2001).

The high mortality in SSc-PAH may be related to excessive collagen content in the heart and the pulmonary arteries. Arterial stiffness is an often overlooked but significant component of pulmonary vascular impedance (PVZ) or right ventricular afterload, and has been linked to right ventricular performance and dysfunction. For a recent review, see (Wang and Chesler 2011). Also, the fact that increased extralobar PA stiffness is currently the best predictor of mortality in all types of PAH (Mahapatra, Nishimura et al. 2006; Gan, Lankhaar et al. 2007; Hemnes and Champion 2008; Hunter, Lee et al. 2008) strongly suggests that PA stiffening strongly contributes to right ventricular failure. We have previously shown that excessive PA collagen accumulation is associated with high-strain PA stiffening (Ooi, Wang et al. 2010). Here, we tested the hypothesis that excessive PA collagen accumulation increases PVZ.

To do so, we measured pulmonary artery pressure and flow waveforms in $Col1a1^{R/R}$ mice and littermate homozygous controls ($Col1a1^{+/+}$) under normoxic conditions, after exposure to chronic hypoxia and after recovery from chronic hypoxia. We measured pulsatile pulmonary artery pressure and flow simultaneously in live mice *in vivo*, which is important because *ex vivo* conditions in which arterial stiffness and PVZ have been measured previously do not exactly reproduce *in vivo* conditions. We also measured large PA size and low-strain stiffness by microcomputed tomography in contrast filled lungs. In both genotypes, we anticipated that chronic hypoxia would increase total pulmonary vascular resistance (Z_0), characteristic impedance (Z_C), pulse wave velocity (PWV) and index of global wave reflections (P_b/P_f). In the $Col1a1^{+/+}$ mice, we anticipated a return to normal values with recovery whereas in the $Col1a1^{R/R}$ mice, we anticipated persistent or further

increases in Z_C and PWV associated with persistent or further increases in PA collagen content.

Methods

Animal Handling

Breeding pairs of Col1a1^{tmJae} mice were obtained from Jackson Laboratory (Bar Harbor, ME). Col1a1$^{+/+}$ and Col1a1$^{R/R}$ mice with a body weight of 23.6±2.7g were randomized into three groups: 63 days of normoxia (normoxia), 42 days of normoxia followed by 21 days of hypoxia (hypoxia), and 21 days of hypoxia followed by 42 days of normoxia (recovery). Mice were randomized so that the same numbers of female and male were in each group. All mice were 17–20 weeks old at the time of euthanization. Animals were housed in hypoxic (FiO_2 = 10% by forced nitrogen) or normoxic conditions as previously described (Ooi, Wang et al. 2010). All procedures were approved by the University of Wisconsin School of Medicine and Public Health and the Zablocki VA Medical Center Animal Care and Use Committees.

In vivo Hemodynamic Measurements

Mice were anesthetized with an intraperitoneal injection of urethane solution (2mg/g body weight), intubated and placed on a ventilator (Harvard Apparatus, Holliston, MA) using a tidal volume of ~225 μL and respiratory rate of ~200 breaths/min. They were then placed supine on a heated pad to maintain body temperature at 38–39°C. A central midline skin incision was made from the lower mandible inferior to the xiphoid process. The thoracic cavity was entered through the sternum, and the chest was carefully removed to expose the right ventricle. In order to confirm the absence of systemic hypertension, the right carotid was cannulated with a 1.2F catheter-tip pressure transducer (Scisense, Inc., London, Ontario, Canada) and advanced into the ascending aorta. Hydroxyethylstarch was used to restore vascular volume due to blood loss as done previously (Tabima, Hacker et al. 2010).

Subsequently, the apex of the right ventricle was localized and a 1.0F pressure-tip catheter (Millar Instruments, Houston, TX) was introduced using a 20 gauge-needle. After instrumentation was established and pressure was stabilized, the catheter was advanced to the main pulmonary artery for measurement. The pressure tracing was recorded at 5 kHz on a hemodynamic workstation (Cardiovascular Engineering, Norwood, MA). The flow measurement was performed via ultrasound (Visualsonics, Toronto, Ontario, Canada) with a 30 MHz probe during catheterization and recorded with the same system. Flow was measured in the main pulmonary artery just distal to the pulmonary valve with the probe in a right parasternal long-axis orientation in the same location as the catheter. The probe was angled until the maximal velocity signal was obtained. Measurement at this point allows for better detection of the main pulmonary artery inner diameter (MPA ID), which we used to convert the flow velocity signal to volume flow rate (Q) assuming a circular orifice. The signals were visually checked for quality and recorded for later analysis.

Pressure and flow waveforms were obtained with mice ventilated with room air. After all measurements were complete, a sample of blood was extracted to measure the hematocrit (Hct).

In vivo Hemodynamic Calculations

Pulmonary arterial flow velocity was calculated by spectral analysis of the digitized broadband Doppler audio signal. The spectral envelope was traced to provide a signal-averaged flow velocity waveform. This flow velocity waveform and the pressure waveform were signal-averaged using the ECG as a fiducial point and then processed and analyzed

using custom software (Cardiovascular Engineering, Norwood, MA). Twenty consecutive cardiac cycles free of extrasystolic beats were selected and averaged.

The diameter of the main pulmonary artery was measured from leading edge to leading edge in B-mode imaging. However, because the MPA is difficult to image technically, we performed an error analysis on MPA ID. We calculated the total uncertainty as the square root of the bias squared plus the precision squared where the bias is the measurement minus the mean for a given group and the precision is provided by the manufacturer of the imaging system (80 μm). In addition, the random error was calculated as the standard deviation divided by the square root of the number of samples (n) times 1.96, for n>30 (Taylor and Kuyatt 1994).

PVZ was calculated using wave intensity analysis as previously described by Mitchell (Mitchell, Pfeffer et al. 1994). Total PVR (Z_0) was calculated as mean PA pressure divided by mean flow rate (i.e., CO). Characteristic impedance (Z_C) was calculated from the ratio of the change in pressure to the change in flow in early ejection. That is, $Z_c = \frac{dP}{dQ}$, where dP and dQ are taken prior to when Q reaches 95% of its maximum value. An assumption inherent in this calculation is that the system is free from reflections because the reflected waves do not have time to return to the proximal bed so early in the cardiac cycle (Mitchell, Pfeffer et al. 1994).

To allow further comparison of our data with parameters commonly used in arterial function analysis, we calculated pulse wave velocity (PWV) from Z_C as $PWV = \frac{Z_C \cdot A}{\rho}$ assuming the density of blood ρ=1060 kg/m^3 and cross-sectional area A=π/4 (MPA ID)^2.

Finally, also based on Z_C, the pulmonary arterial pressure waveform was separated into forward (P_f) and backward (P_b) traveling components using the linear wave separation method (Westerhof, Sipkema et al. 1972). The index of global wave reflections was calculated as the ratio of the amplitude of P_b to P_f.

Pulmonary Arterial Structure and Function

Preparation of mouse lungs for microcomputed tomography (microCT) was performed as previously described (Vanderpool, Kim et al. 2011) in separate groups of Col1a1$^{+/+}$ and Col1a1$^{R/R}$ mice. Briefly, the PA and trachea were cannulated and the lungs ventilated with a mixture of 15% O_2, 6% CO_2, balance nitrogen. After rinsing with a physiological salt solution containing 5% bovine serum albumin, the rho kinase inhibitor Y-27632 was administered (10^{-5} M) to eliminate persistent hypoxic vasoconstriction and then the perfusate was replaced with perfluorooctyl bromide for vascular contrast. Three-dimensional scans were obtained at arterial pressures of 6.3, 7.4, 13.0 and 17.2 mmHg and diameter measurements of the extralobar right pulmonary artery (RPA) and left pulmonary artery (LPA) were made at each pressure as previously described (Vanderpool, Kim et al. 2011). Direct measurements of MPA diameter could not be obtained because of the position of the PA cannula. Nevertheless, to provide a second measurement of MPA diameter to complement the one obtained non-invasively, MPA diameter at a fixed pressure from microCT was estimated from Murray's Law as MPA = (RPA^3 + LPA^3)$^{1/3}$ (Murray 1926).

Based on the microCT measurements of RPA, LPA and MPA, distensibility (α) was calculated as $\alpha = (D_P/D_0 - 1)/P$ where D_P is the luminal diameter at pressure P and D_0 is the luminal diameter at the baseline pressure (here, 6.3 mmHg), assuming a linear pressure vs. diameter relationship over the range of pressures used. Also, compliance (C) was calculated as α times the luminal cross-sectional area at the baseline pressure (Vanderpool, Kim et al.

2011). Note that since wall thickness cannot be measured by microCT, wall stress and elastic modulus could not be calculated.

Hydroxyproline Assay

LPAs were homogenized for measurement of collagen content using a hydroxyproline (OHP) assay (Woessner 1961; Edwards and O'Brien 1980). The procedure is based on alkaline hydrolysis of proteins in the tissue homogenate and monitoring of the free hydroxyproline in hydrolysates after chromophore formation. A standard curve was generated using known amounts of trans-4-hydroxy-L-proline.

Statistical Analysis

For each group, the significances of the overall changes in parameters with exposure were assessed using a two-way analysis of variance (ANOVA, $P<0.05$). When the ANOVA reached statistical significance, Tukey multiple comparisons were used for post hoc analysis. Data were considered significant for P-values less than 0.05. All data are presented in terms of means ± one standard deviation. Statistical analysis was performed using R software (Foundation for Statistical Computing, USA, version 2.6.2).

Results

In Vivo Hemodynamics

In response to hypoxia, PA systolic and diastolic pressures increased in both $Col1a1^{+/+}$ and $Col1a1^{R/R}$ mice (Table 1, $P<0.05$). Mean PA pressure increased by a similar amount in each genotype (~100%). Following 42 days of recovery in normoxic conditions, PA systolic and diastolic pressures of both genotypes returned toward baseline, normoxic values (Table 1). The heart rate under urethane anesthesia was unchanged for all groups except the $Col1a1^{+/+}$ in the recovery condition; systemic pressures in the $Col1a1^{+/+}$ recovery condition tended to be high as a consequence of the higher heart rate.

Neither MPA ID nor CO changed with condition in either $Col1a1^{+/+}$ or $Col1a1^{R/R}$ mice. The maximum total uncertainty in MPA ID measured non-invasively for each group 9.5% and the maximum random error for each group was 3.7%, which, when summed, is less than the standard deviation for each group (~15%).

Hematocrit was significantly increased with hypoxia ($P<0.0005$) and returned close to baseline with recovery in both genotypes (Table 1).

Pulmonary Vascular Impedance

PVZ was analyzed for both genotypes for the three different exposure conditions (normoxia, hypoxia and recovery). In the $Col1a1^{+/+}$ mice, hypoxia increased Z_0 ($P<0.005$), with a return to baseline levels with recovery (Figure 1). A similar increase occurred in the $Col1a1^{R/R}$ mice with hypoxia ($P<0.05$) followed by a similar return to baseline values. Hypoxia did not increase Z_C in either genotype (Figure 2). Recovery decreased Z_C in the $Col1a1^{+/+}$ mice ($p<0.05$) and had no effect in the $Col1a1^{R/R}$ mice (Figure 2). The effects of hypoxia and recovery on PWV were similar to the effects of hypoxia and recovery on Z_C (Figure 3).

The global index of wave reflection calculated as P_b/P_f was not affected by hypoxia or recovery in either $Col1a1^{+/+}$ or $Col1a1^{R/R}$ mice (Figure 4).

Pulmonary Vascular Structure and Function

At a constant pressure of 17.2 mmHg, the inner diameters of the RPA, LPA and MPA did not change with hypoxia or recovery for either genotype (Table 2). The RPA and MPA

tended to be smaller in the Col1a1$^{R/R}$ mice but the difference was not significant. Also, neither distensibility nor compliance changed with either hypoxia or recovery in either mouse type over the pressure range tested: 6.3 to 17.2 mmHg (Table 2).

Collagen Content

Collagen content of Col1a1$^{+/+}$ and Col1a1$^{R/R}$ PAs increased with hypoxia, although the changes only reached significance in the Col1a1$^{+/+}$ mice ($p<0.05$). After recovery, the collagen content of the Col1a1$^{+/+}$ PAs returned to baseline levels, whereas in the Col1a1$^{R/R}$ PAs it continued to increase ($p<0.005$ vs. Normoxia) (Figure 5).

Discussion

The present study demonstrates that 21 days of hypoxia significantly increased Z_0 and collagen content in extralobar pulmonary arteries, but did not change Z_C, PWV or P_b/P_f. Recovery from hypoxia led to decreases in Z_C and PWV below baseline values, and a return of Z_0 to baseline values, in wild type mice. However, in mice with impaired degradation of collagen type I, Z_C and PWV did not decrease with recovery despite a return to baseline Z_0 values. Below, we discuss these novel findings in relation to their implications for pulsatile pulmonary hemodynamics and RV afterload changes in pulmonary hypertension.

Measurements of pulmonary arterial pressure *in vivo* indicate the development of pulmonary hypertension with 21 days of hypoxia in both Col1a1$^{+/+}$ and Col1a1$^{R/R}$ mice as shown with other types of mice by our group and others (Faber, Szymeczek et al. 2007; Weissmann, Hackemack et al. 2009; Tabima, Hacker et al. 2010). Despite a congenital difference in collagen type I metabolism, 17–20 week-old Col1a1$^{+/+}$ and Col1a1$^{R/R}$ mice showed no differences in systolic, diastolic or mean pressures or degree of pulmonary hypertension in response to hypoxia (Table 1). Chronic hypoxia led to a slight increase in aortic pressure, the recovery from which was more complete in Col1a1$^{R/R}$ mice (Table 1). As a consequence, while Z_0 (mPAP/CO) decreased more with recovery in the Col1a1$^{R/R}$ mice than in the Col1a1$^{+/+}$ mice (Figure 1), this finding may be an artifact of the lower aortic pressures in the Col1a1$^{R/R}$ mice. In isolated, ventilated, perfused lung studies using these groups of mice subjected to the same environmental conditions, the decrease in PVR (mPAP minus left atrial pressure divided by CO) with recovery was less dramatic in the Col1a1$^{R/R}$ mice compared to Col1a1$^{+/+}$ mice (unpublished observations).

However, both Z_0 and PVR reflect only the steady, time-averaged components of the pulmonary pressure and flow. A more detailed and global characterization of pulmonary arterial function is the pulmonary vascular impedance, which is affected by the pulsatile, instantaneous as well as the steady, time-averaged components of the pulmonary pressure-flow relationship. As a consequence, PVZ gives information about the effects of wave propagation and reflection. PVZ can be obtained from a spectral analysis of the pulmonary arterial pressure and flow waveforms in the frequency domain or by wave intensity analysis in the time domain. One of the advantages of wave intensity analysis for analyzing PVZ, in contrast to spectral analysis, is that it requires little computation and does not assume the system is at steady-state (Milnor 1989). To our knowledge, ours are the first reported *in vivo* measurements of PVZ in mice.

From PVZ, P_b/P_f, Z_C and PWV can be computed. Whereas P_b/P_f reflects global pulmonary arterial function and thus is more sensitive to intermediate and distal arterial structure and function, Z_C and PWV are typically assumed to be determined by proximal arterial structure and function. For a single, linearly elastic, homogeneous, thin-walled cylindrical artery with no wave reflections, Z_C can be defined as $Z_c = \sqrt{\frac{\rho E h}{2\pi^2 r^5}}$ where E, h, and r are the arterial

elastic modulus, wall thickness and luminal radius, respectively and ρ is the density of blood (Milnor, Conti et al. 1969). Thus, subject to these assumptions, increases in PA diameter and decreases in PA stiffness decrease Z_C with diameter changes having a stronger impact. Alternatively, if Z_C is calculated from waves in which reflections are present, then changes in Z_C and PWV depend on intermediate and distal arterial function as well as proximal arterial function. We saw no evidence of large wave reflections in our pressure and flow rate waveforms in early systole but we cannot rule out small wave reflections from the intermediate or distal vasculature. Changes to the intermediate and distal vasculature that would decrease Z_C and PWV would include increases in diameter and decreases in stiffness.

In both Col1a1$^{+/+}$ and Col1a1$^{R/R}$ mice, 21 days of hypoxia had no effect on Z_C, PWV or P_b/P_f. In previous isolated, ventilated, perfused lung studies on C57BL6 mice, our group has shown that 10 days of hypoxia decreases Z_C because of a greater increase in diameter than stiffness (Tuchscherer, Vanderpool et al. 2007). It is difficult to compare these results to *in vivo* results, however, because the perfusate used in the isolated, ventilated perfused lung preparation has a 3-fold lower viscosity than blood with normal hematocrit, the mean flow rate is 3-fold lower than CO measured *in vivo* and the highest frequency used in the calculation of Z_C *ex vivo* is 5-fold lower than *in vivo*. Indeed, these limitations of the isolated, ventilated, perfused lung preparation motivated the current measurements of PVZ in mice *in vivo*.

Interestingly, in Col1a1$^{+/+}$ mice, Z_C and PWV decreased below baseline levels with recovery from hypoxia, which was unexpected. Since PVZ reflects RV afterload, these decreases in PVZ could be considered an improvement in hemodynamics. Physiologically, there is a precedent for improved hemodynamics after exposure to hypoxia. The benefits of exercise training at altitude are well known (Saunders, Pyne et al. 2009); perhaps even without exercise training, mice adapt to chronic hypoxia in ways that improve pulsatile pulmonary hemodynamics compared to baseline after recovery.

Regardless of the mechanisms of these improved hemodynamics, if the response of Col1a1$^{+/+}$ mice to hypoxia and recovery is normal, then the responses of Col1a1$^{R/R}$ mice can be considered abnormal, and dependent on vascular collagen content. Thus, the constancy of Z_C and PWV from hypoxia to recovery in the Col1a1$^{R/R}$ mice may reflect impaired pulmonary vascular remodeling due to excessive collagen accumulation, the specific features of which remain to be elucidated.

It is important to note a few limitations of this study. We previously demonstrated large PA stiffening by isolated vessel experiments in Col1a1$^{+/+}$ and Col1a1$^{R/R}$ mice after only 10 days of hypoxia (Ooi, Wang et al. 2010). However, simultaneous studies in C57BL6 mice showed relatively mild remodeling in the pulmonary arteries as measured by microCT after 10 days of hypoxia (Vanderpool, Kim et al. 2011). Therefore, in this study we lengthened the hypoxia exposure. Yet, even this longer exposure time did not lead to PA stiffening measurable by our microCT techniques, which we now suspect is related to the relatively low pressures used. Also, our previous tests demonstrated nearly complete pressure recovery after 32 days. Therefore, we shortened the recovery time in these studies. We acknowledge that changing the hypoxia and recovery times makes comparison to our prior work difficult and leaves us without direct evidence of large PA stiffening in association with excessive PA collagen accumulation after 21 days of hypoxia.

Also, the mean aortic pressures measured here (Table 1) are well below ambulatory values reported for awake mice at heart rates of 450–500 bpm (93–103 mmHg) or 600–650 bpm (110–124 mmHg) (Hoyt, Hawkins et al. 2007). They are also below mean aortic pressures measured invasively in mice anesthetized with isoflurane that had heart rates of 470–620

bpm (81–105 mmHg) (Pacher, Nagayama et al. 2008). Independent of changes in cardiac output, poor thermoregulation can lower systemic pressures (unpublished observation; D. Tabima) but whether this played a role in the current results must await further investigation.

In summary, here we present novel pulmonary vascular impedance measurements obtained in mice *in vivo*, which allow us to quantify the impact of pulmonary vascular remodeling on right ventricular afterload, which is critical to outcomes in pulmonary hypertension. Our results show that proximal artery collagen accumulation does not alter pulsatile pulmonary hemodynamic parameters measured *in vivo*, including characteristic impedance, pulse wave velocity and global wave reflection. However, excessive collagen accumulation does prevent decreases in characteristic impedance and pulse wave velocity with recovery from hypoxia. The clinical implications of these findings for SSc-PAH and other types of PH in which collagen mediates pulmonary artery structure and function changes remain to be elucidated.

Acknowledgments

The present study was supported in part by DNP-Fulbright-Colciencias program and Universidad de los Andes-Colombia (DMT) and National Institutes of Health grant R01HL086939 (NCC). We also thank Larry Whitesell and Guoqing Song for performing *in vivo* hemodynamics measurements and Dr. Lian Tian for constructive comments on this manuscript.

References

Champion HC, Villnave DJ, et al. A novel right-heart catheterization technique for in vivo measurement of vascular responses in lungs of intact miceAmerican. Journal of Physiology-Heart and Circulatory Physiology. 2000; 278(1):H8–H15.

Coghlan JG, Mukerjee D. The heart and pulmonary vasculature in scleroderma: clinical features and pathobiology. Curr Opin Rheumatol. 2001; 13(6):495–499. [PubMed: 11698727]

Cotran, RS.; Kuman, V., et al. Robbins Pathologic Basis of Disease. Philadelphia: W. B. Saunders; 1999.

Edwards CA, O'Brien WD Jr. Modified assay for determination of hydroxyproline in a tissue hydrolyzate. Clinica chimica acta; international journal of clinical chemistry. 1980; 104(2):161–167.

Faber JE, Szymeczek CL, et al. Alpha1-adrenoceptor-dependent vascular hypertrophy and remodeling in murine hypoxic pulmonary hypertension. Am J Physiol Heart Circ Physiol. 2007; 292(5):H2316–2323. [PubMed: 17220188]

Fagan KA, Badesch DB. Pulmonary hypertension associated with connective tissue disease. Prog Cardiovasc Dis. 2002; 45(3):225–234. [PubMed: 12525998]

Gan CT, Lankhaar JW, et al. Noninvasively assessed pulmonary artery stiffness predicts mortality in pulmonary arterial hypertension. Chest. 2007; 132(6):1906–1912. [PubMed: 17989161]

Hemnes AR, Champion HC. Right heart function and haemodynamics in pulmonary hypertension. International journal of clinical practice. 2008; (160):11–19. [PubMed: 18638171]

Hoyt, RF.; Hawkins, JV., et al. Mouse Physiology. In: Fox, JG.; Barthold, SW.; Davisson, MT., et al., editors. The Mouse in Biomedical Research: Normative biology, husbandry and models. Sand Diego, CA: Academic Press; 2007. p. 3

Hunter KS, Lee PF, et al. Pulmonary vascular input impedance is a combined measure of pulmonary vascular resistance and stiffness and predicts clinical outcomes better than pulmonary vascular resistance alone in pediatric patients with pulmonary hypertension. American Heart Journal. 2008; 155(1):166–174. [PubMed: 18082509]

Kobs RW, Chesler NC. The mechanobiology of pulmonary vascular remodeling in the congenital absence of eNOS. Biomechanics and modeling in mechanobiology. 2006; 5(4):217–225. [PubMed: 16520964]

Kobs RW, Chesler NC. The mechanobiology of pulmonary vascular remodeling in the congenital absence of eNOS. Biomech Model Mechanobiol. 2006; 5(4):217–225. [PubMed: 16520964]

Kobs RW, Muvarak NE, et al. Linked mechanical and biological aspects of remodeling in mouse pulmonary arteries with hypoxia-induced hypertension. Am J Physiol Heart Circ Physiol. 2005; 288(3):H1209–1217. [PubMed: 15528223]

Mahapatra S, Nishimura RA, et al. The prognostic value of pulmonary vascular capacitance determined by Doppler echocardiography in patients with pulmonary arterial hypertension. Journal of the American Society of Echocardiography : official publication of the American Society of Echocardiography. 2006; 19(8):1045–1050. [PubMed: 16880101]

Milnor, WR. Hemodynamics. Baltimore: Williams & Wilkins; 1989.

Milnor WR, Conti CR, et al. Pulmonary arterial pulse wave velocity and impedance in man. Circulation research. 1969; 25(6):637–649. [PubMed: 5364641]

Mitchell GF, Pfeffer MA, et al. Measurement of aortic input impedance in rats. The American Journal of Physiology. 1994; 267(5 Pt 2):H1907–1915. [PubMed: 7977821]

Murray CD. The Physiological Principle of Minimum Work Applied to the Angle of Branching of Arteries. J Gen Physiol. 1926; 9(6):835–841. [PubMed: 19872299]

Ooi CY, Wang Z, et al. The role of collagen in extralobar pulmonary artery stiffening in response to hypoxia-induced pulmonary hypertension. Am J Physiol Heart Circ Physiol. 2010

Ooi CY, Wang Z, et al. The role of collagen in extralobar pulmonary artery stiffening in response to hypoxia-induced pulmonary hypertension. Am J Physiol Heart Circ Physiol. 2010; 299(6):H1823–1831. [PubMed: 20852040]

Pacher P, Nagayama T, et al. Measurement of cardiac function using pressure-volume conductance catheter technique in mice and rats. Nat Protoc. 2008; 3(9):1422–1434. [PubMed: 18772869]

Salerni R, Rodnan GP, et al. Pulmonary hypertension in the CREST syndrome variant of progressive systemic sclerosis (scleroderma). Ann Intern Med. 1977; 86(4):394–399. [PubMed: 848800]

Saunders PU, Pyne DB, et al. Endurance training at altitude. High Alt Med Biol. 2009; 10(2):135–148. [PubMed: 19519223]

Schwenke DO, Pearson JT, et al. Imaging of the pulmonary circulation in the closed-chest rat using synchrotron radiation microangiography. J Appl Physiol. 2007; 102(2):787–793. [PubMed: 17038493]

Silver RM. Scleroderma. Clinical problems. The lungs. Rheum Dis Clin North Am. 1996; 22(4):825–840. [PubMed: 8923598]

Simonneau G, Galie N, et al. Clinical classification of pulmonary hypertension. Journal of the American College of Cardiology. 2004; 43(12 Suppl S):5S–12S. [PubMed: 15194173]

Sonobe T, Schwenke DO, et al. Imaging of the closed-chest mouse pulmonary circulation using synchrotron radiation microangiography. J Appl Physiol. 2011; 111(1):75–80. [PubMed: 21527665]

Stenmark KR, Davie N, et al. Role of the adventitia in pulmonary vascular remodeling. Physiology (Bethesda, Md). 2006; 21:134–145.

Stenmark KR, Fagan KA, et al. Hypoxia-induced pulmonary vascular remodeling: cellular and molecular mechanisms. Circulation research. 2006; 99(7):675–691. [PubMed: 17008597]

Stenmark KR, Mecham RP. Cellular and molecular mechanisms of pulmonary vascular remodeling. Annual Review of Physiology. 1997; 59:89–144.

Tabima DM, Chesler NC. The effects of vasoactivity and hypoxic pulmonary hypertension on extralobar pulmonary artery biomechanics. J Biomech. 2010; 43(10):1864–1869. [PubMed: 20416876]

Tabima DM, Hacker TA, et al. Measuring right ventricular function in the normal and hypertensive mouse hearts using admittance-derived pressure-volume loops. Am J Physiol Heart Circ Physiol. 2010

Tabima DM, Hacker TA, et al. Measuring right ventricular function in the normal and hypertensive mouse hearts using admittance-derived pressure-volume loops. Am J Physiol Heart Circ Physiol. 2010; 299(6):H2069–2075. [PubMed: 20935149]

Taylor BN, Kuyatt CE. Guidelines for evaluating and expressing the uncertainty of NIST measurement results. 1994

Tuchscherer HA, Vanderpool RR, et al. Pulmonary vascular remodeling in isolated mouse lungs: effects on pulsatile pressure-flow relationships. Journal of Biomechanics. 2007; 40(5):993–1001. [PubMed: 16756983]

Vanderpool RR, Kim AR, et al. Effects of acute Rho kinase inhibition on chronic hypoxia-induced changes in proximal and distal pulmonary arterial structure and function. J Appl Physiol. 2011; 110(1):188–198. [PubMed: 21088209]

Wang Z, Chesler N. Pulmonary Vascular Wall Stiffness: An Important Contributor to the Increased Right Ventricular Afterload with Pulmonary Hypertension. Pulmonary Circulation. 2011; 1(2)

Weissmann N, Hackemack S, et al. The soluble guanylate cyclase activator HMR1766 reverses hypoxia-induced experimental pulmonary hypertension in mice. Am J Physiol Lung Cell Mol Physiol. 2009; 297(4):L658–665. [PubMed: 19617308]

Westerhof N, Sipkema P, et al. Forward and backward waves in the arterial system. Cardiovascular research. 1972; 6(6):648–656. [PubMed: 4656472]

Woessner JF Jr. The determination of hydroxyproline in tissue and protein samples containing small proportions of this imino acid. Archives of Biochemistry and Biophysics. 1961; 93:440–447. [PubMed: 13786180]

Young RH, Mark GJ. Pulmonary vascular changes in scleroderma. Am J Med. 1978; 64(6):998–1004. [PubMed: 148843]

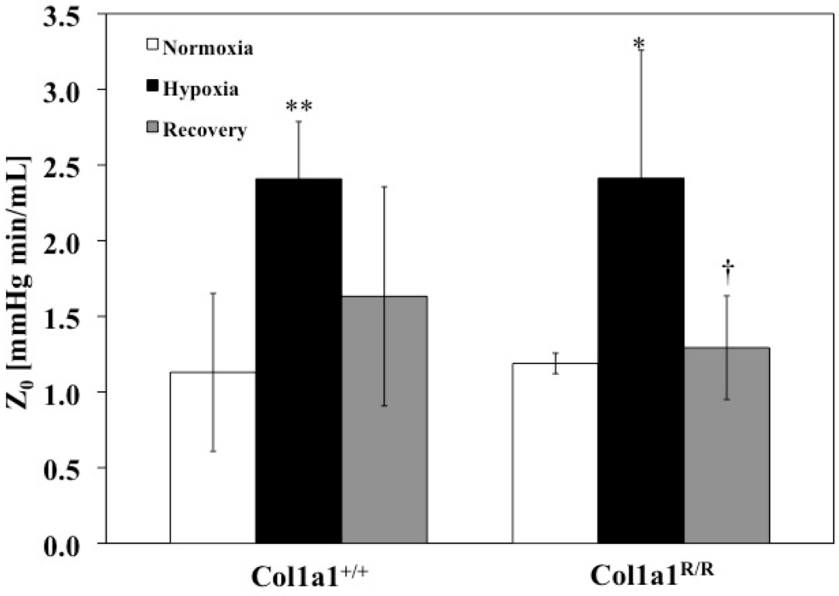

Figure 1.

Z_0 increased significantly with hypoxia and returned close to baseline, normoxic levels with Recovery in both genotypes. * $p<0.05$ vs. Normoxia; ** $p<0.005$ vs. Normoxia; † $p<0.05$ vs. Hypoxia. Sample sizes for each group (Normoxia, Hypoxia, Recovery) were, for Col1a1$^{+/+}$: 7, 5, 7; and for Col1a1$^{R/R}$: 7, 5, 5, respectively.

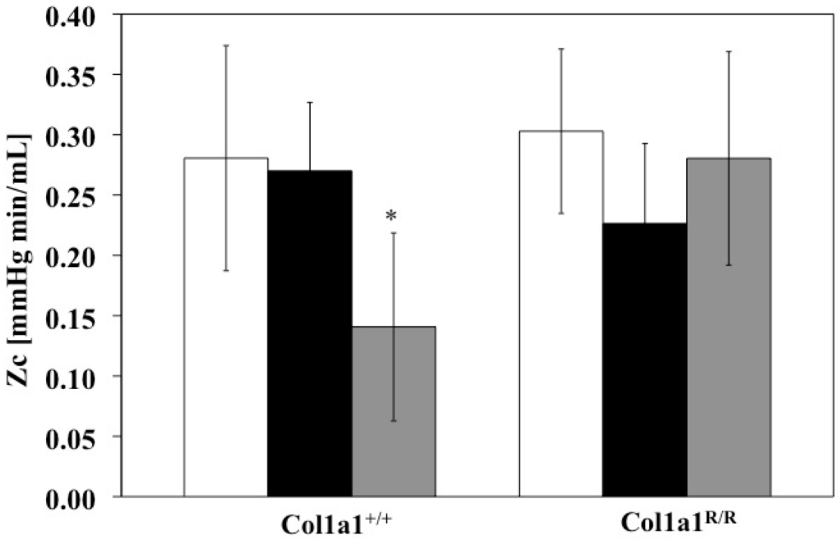

Figure 2.

Z_C did not increase with hypoxia in either genotype but did decrease with Recovery in the Col1a1$^{+/+}$ mice. * $p<0.05$ vs. Normoxia. Sample sizes for each group (Normoxia, Hypoxia, Recovery) were, for Col1a1$^{+/+}$: 7, 5, 7; and for Col1a1$^{R/R}$: 7, 5, 5, respectively.

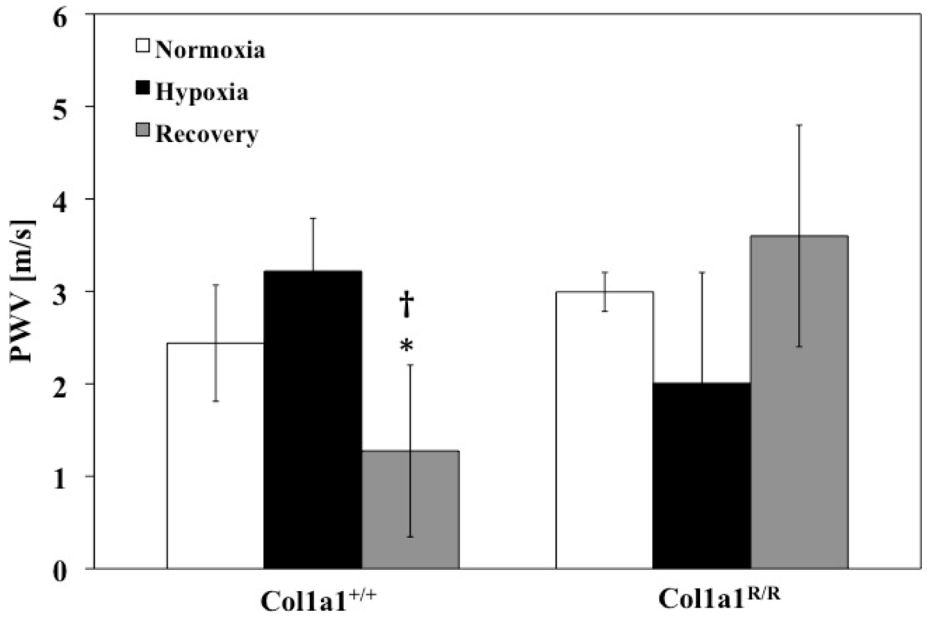

Figure 3.

PWV did not increase with hypoxia in either genotype but did decrease with recovery in the Col1a1$^{+/+}$ mice. * $p<0.05$ vs. Normoxia; † $p<0.05$ vs. Hypoxia. Sample sizes for each group (Normoxia, Hypoxia, Recovery) were, for Col1a1$^{+/+}$: 7, 5, 7; and for Col1a1$^{R/R}$: 7, 5, 5, respectively.

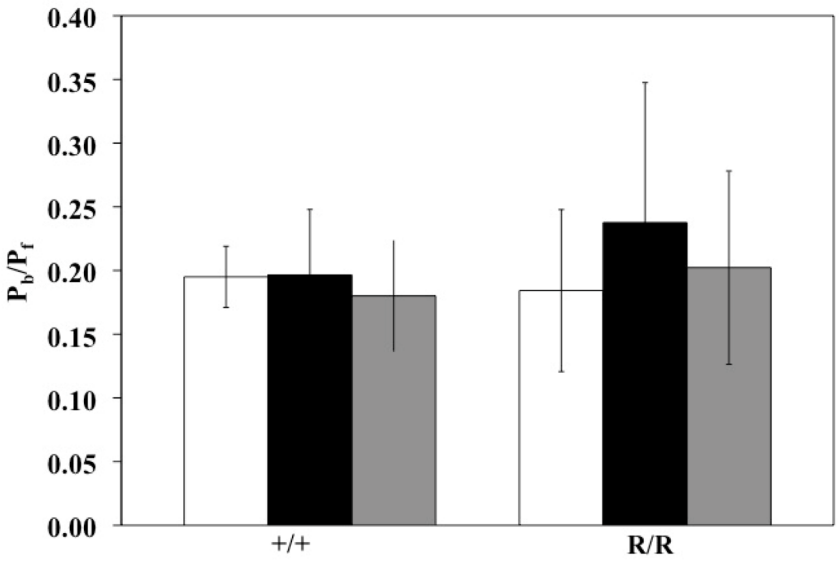

Figure 4.

Global index of wave reflection (P_b/P_f) did not change with hypoxia or recovery in either genotype. Sample sizes for each group (Normoxia, Hypoxia, Recovery) were, for $Col1a1^{+/+}$: 7, 5, 7; and for $Col1a1^{R/R}$: 7, 5, 5, respectively.

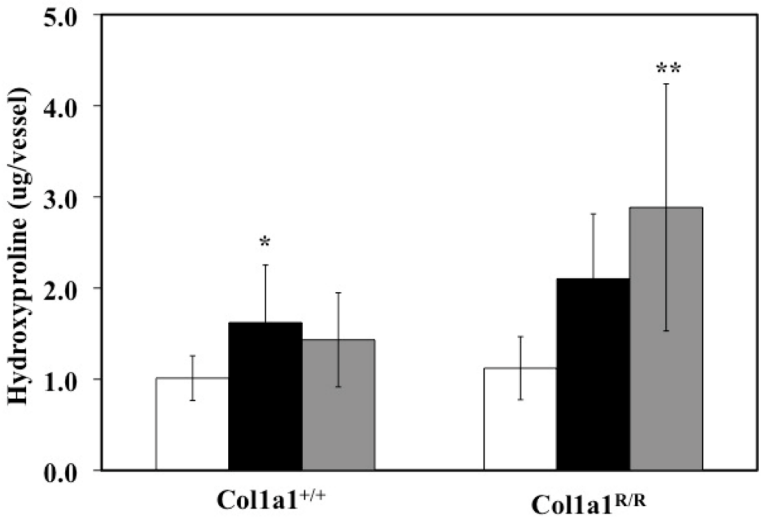

Figure 5.

Extralobar PA collagen content increased with hypoxia in the Col1a1$^{+/+}$ mice and increased further with recovery in the Col1a1$^{R/R}$ mice as measured via hydroxyproline (OHP) content. * $p<0.05$ vs. Normoxia, ** $p<0.005$ vs. Normoxia. Sample sizes for each group (Normoxia, Hypoxia, Recovery) were, for Col1a1$^{+/+}$: 8, 5, 7; and for Col1a1$^{R/R}$: 9, 4, 5, respectively.

Table 1

Pulmonary arterial (PA) pressures, aortic pressures, heart rate (HR), PA inner diameter, cardiac output (CO) and hematocrit (Hct).

		Col1a1$^{+/+}$			Col1a1$^{R/R}$		
		Normoxia (n=7)	**Hypoxia (n=5)**	**Recovery (n=7)**	**Normoxia (n=7)**	**Hypoxia (n=5)**	**Recovery (n=5)**
PA pressure [mm Hg]	**Systolic**	19±3	31± 5*	26± 7	20±5	33±5*	22±7†
	Diastolic	7±4	18± 3***	15± 6*	8±3	20±5**	11±6†
	Mean	11±3	23± 3***	19± 7*	13±3	25±5***	15±6†
Aortic pressure [mm Hg]	**Systolic**	73±24	82±37	84±19	72±25	69±28	56±5
	Diastolic	24±11	41±13	49±17	20±14	40±14	12±5
	Mean	39± 5	50±12	59±19	35±6	45±19	25±3
HR [bpm]		540±45	562±47	617±28*	540±48	569±63	530± 53
MPA inner diam. [mm]		1.3±0.2	1.3±0.2	1.4±0.1	1.3±0.2	1.4±0.2	1.4±0.1
CO [ml/min]		11±3	9±2	11±2	10±3	12±5	9±3
Hct [−]		60± 6	81± 5***	51± 4†††	56±4	85±4***	57±7†††

*p<0.05 vs. Normoxia,

**p<0.005 vs. Normoxia,

***p<0.0005 vs. Normoxia,

†p<0.05 vs. Hypoxia,

†††p<0.0005 vs. Hypoxia.

Table 2

Right and left extralobar PA inner diameter (RPA and LPA, respectively) measured by microCT at a perfusion pressure of 17 mmHg and main PA (MPA) inner diameter computed from these by Murray's Law. Distensibility (α) and compliance (C) for RPA, LPA and MPA over the pressure range 6.3 to 17.2 mmHg.

		Col1a1$^{+/+}$			Col1a1$^{R/R}$		
		Normoxia (n=3)	**Hypoxia (n=5)**	**Recovery (n=5)**	**Normoxia (n=4)**	**Hypoxia (n=5)**	**Recovery (n=4)**
ID	**RPA [mm]**	1.29±0.31	1.26±0.17	1.31±0.21	1.04±0.07	1.10±0.07	1.17±0.04
	LPA [mm]	0.92±0.16	0.90±0.11	0.94±0.15	0.85±0.05	0.80±0.09	0.86±0.04
	MPA [mm]	1.43±0.32	1.39±0.18	1.46±0.23	1.20±0.08	1.23±0.09	1.31±0.05
α	**RPA [1/mmHg]**	0.030±0.008	0.020±0.001	0.030±0.010	0.020±0.004	0.020±0.005	0.025±0.004
	LPA [1/mmHg]	0.030±0.005	0.020±0.007	0.030±0.009	0.020±0.003	0.020±0.010	0.020±0.004
	MPA [1/mmHg]	0.032±0.007	0.016±0.08	0.030±0.05	0.020±0.003	0.030±0.005	0.020±0.004
C	**RPA [mm^2/mmHg]**	0.016±0.005	0.015±0.006	0.024±0.017	0.009±0.002	0.008±0.002	0.013±0.001
	LPA [mm^2/mmHg]	0.008±0.002	0.007±0.002	0.012±0.008	0.006±0.002	0.004±0.002	0.007±0.001
	MPA [mm^2/mmHg]	0.022±0.01	0.011±0.007	0.016±0.003	0.012±0.0015	0.017±0.001	0.014±0.002